Sedimentary Geology 208 (2008) 36–44

Contents lists available at ScienceDirect

Sedimentary Geology

journal homepage: www.elsevier.com/locate/sedgeo

Proximal provenance of the western Songpan–Ganzi turbidite complex (Late Triassic, eastern Tibetan plateau): Implications for the tectonic amalgamation of China

Kai-Jun Zhang [a,b,*], Bing Li [a,c], Qing-Guo Wei [a,c], Jian-Xin Cai [a,c], Yu-Xiu Zhang [a,c,d]

[a] Guangzhou Institute of Geochemistry, Key Laboratory of Geology of Marginal Sea, Chinese Academy of Sciences, Wushan, Guangzhou 510640, China
[b] Department of Earth Sciences, Nanjing University, Nanjing 210093, China
[c] Graduate School, Chinese Academy of Sciences, Beijing 100008, China
[d] Research Center for Tibetan Plateau Geology and School of the Earth Sciences and Resources, China University of Geosciences at Beijing, Beijing 100083, China

ARTICLE INFO

Article history:
Received 1 July 2007
Received in revised form 17 March 2008
Accepted 17 April 2008

Keywords:
Turbidite
Collisional orogen
Qiangtang
Songpan–Ganzi
Tibet
Upper Triassic

ABSTRACT

The Late Triassic Songpan–Ganzi turbidite complex on the eastern Tibetan plateau, which covers an area of ~2.2×10^5 km^2, is one of the largest flysch turbiditic basins on Earth. It is juxtaposed with major Chinese continental blocks across several outstanding Tethyan sutures, and is critical to elucidating the tectonic amalgamation of China. However, the provenance of the turbidites remains the subject of intense debate. Detrital modes and heavy-mineral spectra of sandstone samples from three turbidite profiles in the western Songpan–Ganzi complex were determined in an attempt to elucidate their provenance and the type of tectonic setting in which they were deposited. Upper Triassic turbidites in the western Songpan–Ganzi complex have an overwhelming derivation from an orogen source, as shown by the average framework compositions of the sandstones ($Q_{57}F_{21}L_{22}$, $Qm_{52}F_{21}Lt_{27}$, $Qp_{23}Lvm_0Lsm_{77}$). The compositional and textural immaturity of the sandstones suggests limited transport and nearby sources. Both light and heavy mineral and lithic fractions indicate dominant metamorphic source rocks and subordinate ophiolitic and sedimentary source rocks. The occurrence of C-type garnet, omphacite, rutile, and Si-rutile, and the high-silica content of phengites reveal that the source rocks underwent ultrahigh-pressure conditions. Therefore, we advocate that the western Songpan–Ganzi Late Triassic turbidites were derived from nearby central Qiangtang Triassic collisional orogen sources, rather than distant Dabie–Qinling sources eroded after North China–South China collision, as previously proposed. The analogy of the Songpan–Ganzi turbidites to the Bengal–Indus fans is not favored. The central Qiangtang metamorphic belt is unlikely to have occurred as an early Mesozoic mélange underthrust from the Jinsa suture, and is more likely to have been an in situ Triassic ultrahigh-pressure orogen. Our provenance interpretation implies that the Paleotethys, represented by the present Jinsa and Kunlun sutures, was not yet closed when central Qiangtang was being exhumed to supply the sediments of the Songpan–Ganzi basin. This challenges the conventional model for sequential amalgamation of China during the Phanerozoic.

1. Introduction

The Songpan–Ganzi complex in the eastern Tibetan plateau is one of the largest flysch turbiditic basins on Earth. It contains succession with an average thickness of up to 10 km accumulated during Ladinian through Norian times (~230–203 Ma) (Huang and Chen, 1987), and covers ~2.2×10^5 km^2 of central China (Fig. 1; Nie et al., 1994; Zhou and Graham, 1996). This triangular terrain is juxtaposed with major Chinese continental blocks across several outstanding Tethyan sutures in central-western China (e.g. Huang and Chen, 1987; Zhang, 2001b, 2002. Fig. 1A), and may hold answers to many critical questions about the tectonic amalgamation of China (Zhou and Graham, 1996). However, the provenance of the turbidites still remains the subject of intense debate. They have been interpreted to be sourced from (1) exhumation of the Dabie ultrahigh-pressure (UHP) metamorphic rocks in eastern China (Nie et al., 1994); (2) the Qinling–Dabie orogen between the North China and South China blocks (Zhou and Graham, 1996; Weislogel et al., 2006); (3) the Kunlun arc north of the Songpan–Ganzi complex (Gu, 1994; She et al., 2006); and (4) the North and South China blocks (Bruguier et al., 1997). More recently, Zhang et al. (2006a) postulated that at least the western Songpan–Ganzi turbidites represent material eroded during exhumation of the central Qiangtang UHP metamorphic rocks (Fig. 1), based on volumetric comparisons between the Songpan–Ganzi complex and the amount of material removed to exhume UHP rocks, and on Late Triassic (~220–202 Ma) metamorphic cooling ages of the central Qiangtang UHP rocks (Kapp et al., 2000, 2003).

* Corresponding author. Guangzhou Institute of Geochemistry, Key Laboratory of Geology of Marginal Sea, Chinese Academy of Sciences, Wushan, Guangzhou 510640, China. Tel.: +86 20 85290232; fax: +86 20 85290231.
E-mail addresses: kaijun@gig.ac.cn, kjzhang@nju.edu.cn, okaijun@yahoo.com.cn (K.-J. Zhang).

0037-0738/$ – see front matter © 2008 Elsevier B.V. All rights reserved.
doi:10.1016/j.sedgeo.2008.04.008

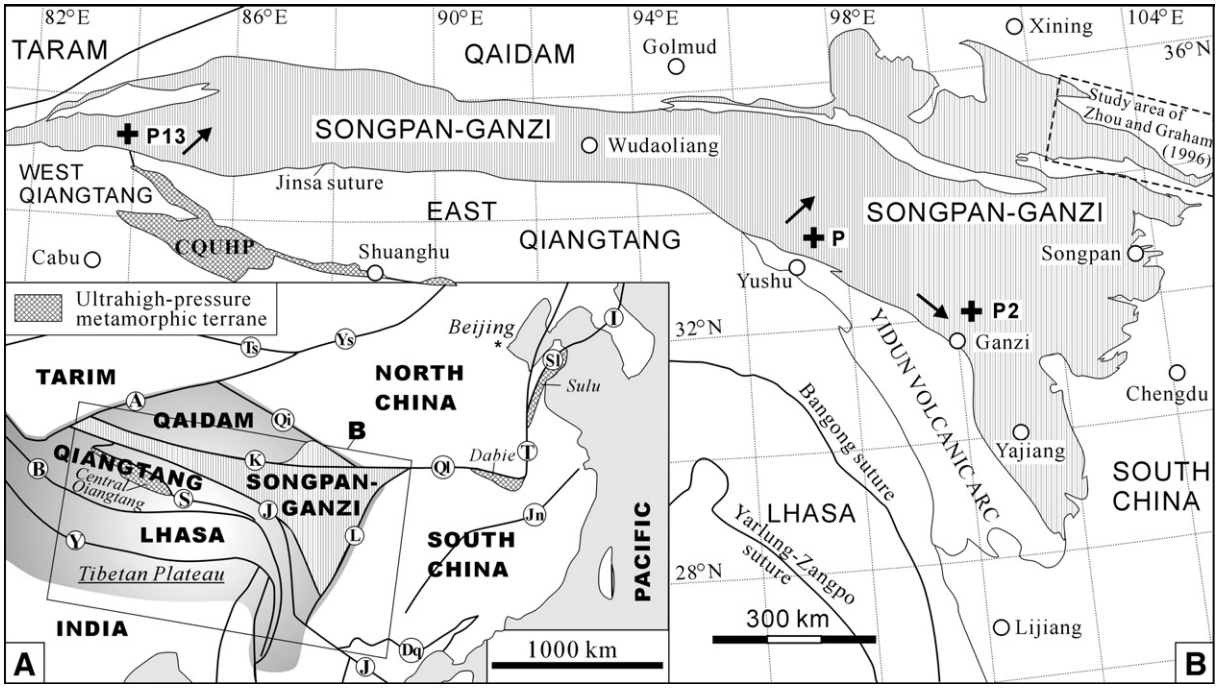

Fig. 1. A: Sketch tectonic map of eastern Asia, revised after Zhang et al. (2006d), and the location of the Songpan–Ganzi complex is also shown. Main sutures or faults: *A*—Altyan fault zone, *B*—Bangong–Nujiang suture, *Dq*—Dian-Qiong suture, *I*—Imjingang fault zone, *J*—Jinsa suture, *Jn*—Jiangnan suture, *K*—Kunlun suture, *L*—Longmenshan fault zone, *Qi*—Qilian suture, *Ql*—Qinling suture, *S*—Shuanghu suture, *Sl*—Sulu ultrahigh-pressure (UHP) belt, *T*—Tanlu fault zone, *Ts*—Tianshan suture, *Y*—Yarlung Zangbo suture, *Ys*—Yinshan suture. B: Locations of profiles (black crosses) within the Songpan–Ganzi complex, simplified after GSC and CIGMR (2004). Also shown is the study area of Zhou and Graham (1996). Black arrows represent average restored paleocurrent orientations. *CQUHP*—central Qiangtang UHP belt.

Compared with the enormous area of the Songpan–Ganzi terrain, broad reconnaissance investigations of the geology of this huge terrain have been restricted to its northeastern corner. For the remainder, especially northern-western part, little information is available to constrain the origin of the turbidites. Conventional sandstone provenance signatures of the Songpan–Ganzi turbidites are still distinguishable (Zhou and Graham, 1996; this study), even though zeolite- to pumpellyite-grade metamorphism overprinted Songpan–Ganzi strata during latest Triassic–Early Jurassic time (Bruguier et al., 1997). Data from detrital modes of sandstones often provide key information in provenance determination (e.g., Ingersoll and Suczek, 1979; Dickinson et al., 1983; Ingersoll et al., 1984; Suczek and Ingersoll, 1985; Najman, 2006). Here, we present 60 sandstone compositions coupled with eight dense mineral measurements that shed new light on the origin of the northern-western Songpan–Ganzi complex and its link to the central Qiangtang orogen unroofing.

2. Methods

About 250 sandstone samples were collected from three Upper Triassic stratigraphic profiles, basically representative of typical lithologies (Fig. 2). Paleocurrent indicators were also measured from sampled outcrops and from other outcrops where such indicators were accessible. The petrography of 60 samples with <25% matrix was determined by point-counting 414–717 points per thin section. Medium- to coarse-grained sandstones were analyzed using the Gazzi–Dickinson method to minimize grain-size effects (Dickinson et al., 1983; Ingersoll et al., 1984). Modal compositions are listed in Table 1.

Eight medium-grained sandstone samples were selected for conventional heavy-mineral analysis. Separation and preparation of heavy minerals followed standard procedures described by Mange and Maurer (1992). Heavy minerals were identified using standard petrographic procedures. Two hundred grains from each sample were counted as described by Mange and Maurer (1992). Morphologies of single grains were examined by scanning electron microscopy. Selected dense minerals were then adhered to targets using epoxy resins and ground and polished for electron microprobe analyses. The heavy-mineral spectra are summarized in Table 2, and the chemistry of minerals is presented in Table 1 in the Online supplementary data, respectively.

Electron microprobe analyses of minerals from both thin-sections and targets were performed using a Jeol JXA-8100 instrument at the Guangzhou Institute of Geochemistry, Chinese Academy of Science (GIGCAS), operated at 15 kV accelerating potential, 30 nA beam current, and 20 s counting time. Final results were reduced by a ZAF correction program. The Fe^{2+}/Fe^{3+} ratios in omphacites were calculated normalizing the analyses to four cations and six oxygens, following the methods of Ryburn et al. (1976).

3. Detrital modes

Texturally, the sandstones are immature typical first-cycle sandstones; grains are angular to subangular, and there are few clasts that suggest recycling. The sandstones are poorly sorted, and have a muddy matrix and a very low porosity (Fig. 3). The matrix is dominantly pseudomatrix and represents deformed fine-grained lithic grains, perhaps overwhelmingly originating from metamorphic rocks. Quartz is the most abundant component in these samples (Fig. 4; Table 1), with absolute abundances ranging from 30% to 86% (mean of 57 ± 14%). Monocrystalline quartz is far more plentiful than polycrystalline quartz, with averages of 52% and 5%, respectively. Quartz with undulose extinction (~90%) is markedly more common than fragments with straight extinction. Chert also occurred a ubiquitous constituent of the sandstones (Fig. 3B), with an average up to 1.3% (Table 1). Lithic fragments make up an average of 27% of the sandstones. These lithics are overwhelmingly of metamorphic source

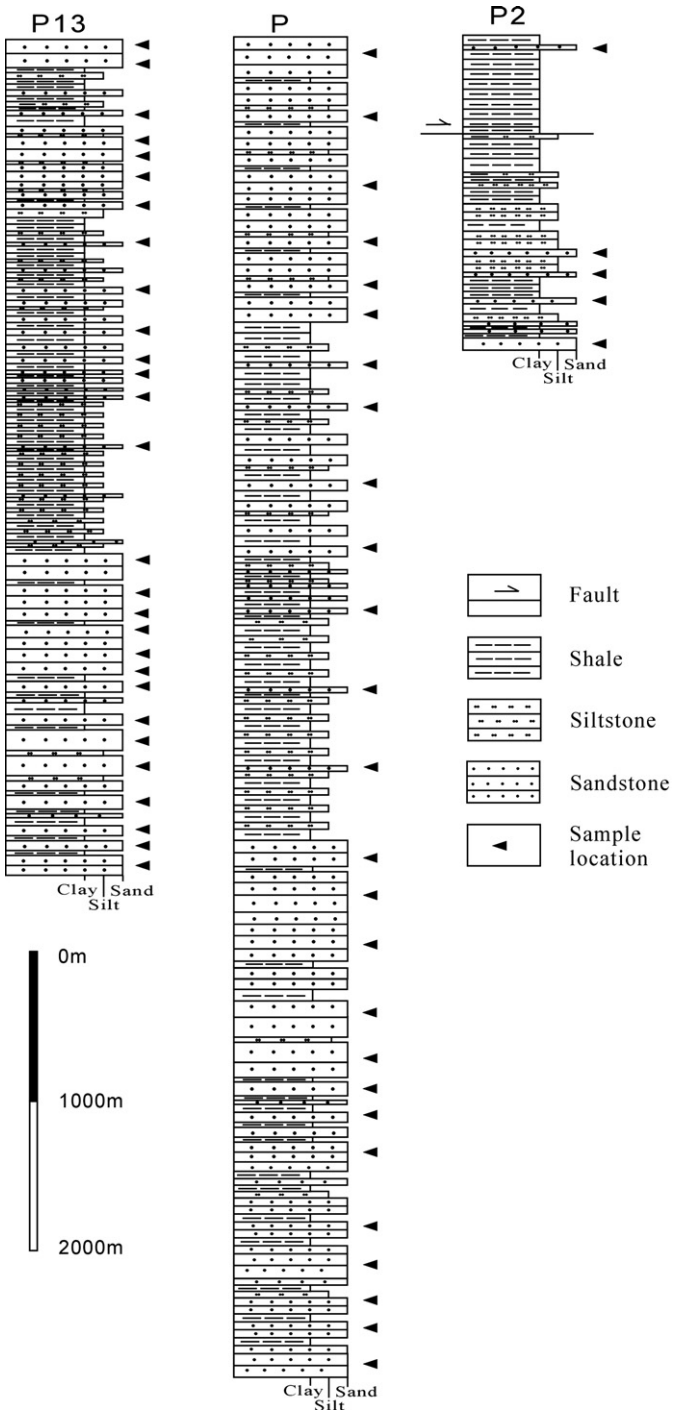

Fig. 2. Stratigraphic columns for the three profiles with the sample locations indicated. See Fig. 1B for the locations of the three profiles.

(schistose, along with minor slate and phyllite fragments, Fig. 3C) and only a few basaltic volcanic fragments (<0.2%) were found in limited sandstone samples. Feldspars, dominated by albite (generally Ab >90%; Table 1 in the Online supplementary data) with intense sericitization, constitute 21 (±14) % of framework grains on average, but show a striking contrast in amount in various samples, with a range varying from 6 to 55%. Some albites are associated with flexural twins (Fig. 5A), indicating their parent rocks must have undergone ductile deformation under high temperature and high pressure. Alkali feldspar grains (dominantly microcline and perthite. Fig. 3B) also constitute a small but significant component with an average of ~3% of the sandstones. Mica grains are abundant, forming a maximum of 7% of the framework compositions. These single micas and those in metamorphic lithics are dominantly phengites, with SiO_2 content of >47% and Si cations of 3.0–3.4 per 11 oxygens (Fig. 6; Table 1 in the Online supplementary data). In those samples from which Si-intermediate phengites were recovered, mica and metamorphic lithic fragments are particularly abundant. Carbonate grains are common and generally well-rounded (Fig. 3B). There is a distinct spatial variation of the framework-grain assemblage. The westernmost profile (P13) has a lower chert content (average ~0.5%) than its

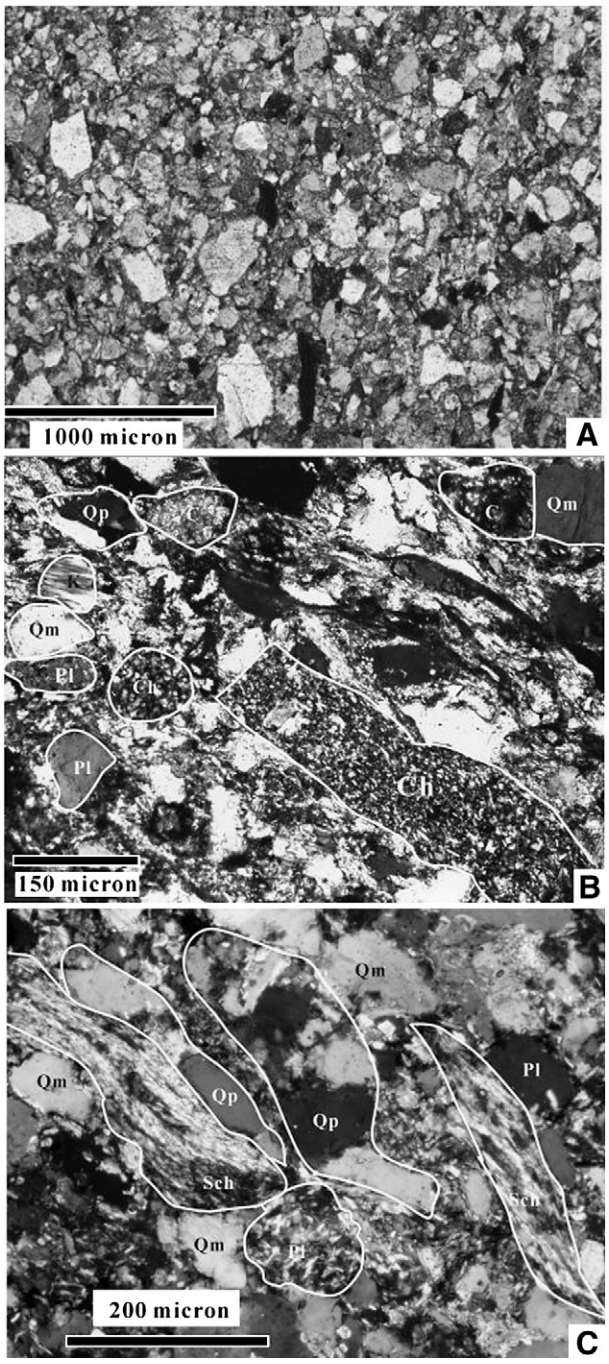

Fig. 3. Photos characterizing the detrital modes of the sandstones from Triassic flysch sequence in the western Songpan–Ganzi complex. Photo A was taken from profile P13; B from profile P, C from profile P2. Abbreviations: *C*—carbonate, *Cl*—chlorite, *K*—K-feldspar, *Pl*—plagioclase, *Qm*—monocrystalline quartz, *Qp*—polycrystalline quartz, *Sch*—Schist. Photo A with single polar, and B and C with crossed polars.

Table 1
Compositions of Late Triassic sandstones from the western Songpan–Ganzi complex

Sample	Matrix	Qm	Qp′	Chert	Plagioclase	K-Feldspar	Ls	Carbonate	Lm	Lv	Phyllosicilate	Dense minerals	Total	Q (%)	F (%)	L (%)	Qm (%)	F (%)	Lt (%)	Qp (%)	Lv (%)	Lsm (%)
Profile P in Fig. 1B (33°07′06″N, 97°20′02″E)																						
P-1	88	177	19	8	74	5	10	61	65	0	5	4	515	57	22	21	50	22	28	27	0	73
P-2	46	314	11	0	17	18	0	28	28	1	22	0	484	84	9	7	81	9	10	28	3	70
P-3	47	299	13	0	13	20	0	39	41	0	10	0	482	81	9	11	77	9	14	24	0	76
P-4	23	322	12	0	9	16	1	29	42	0	12	0	465	83	6	11	80	6	14	22	0	78
P-5	47	268	10	7	30	37	0	32	43	0	23	4	500	72	17	11	68	17	15	29	0	71
P-6	72	194	37	0	18	19	2	52	91	0	6	2	492	64	10	26	54	10	36	29	0	71
P-7	156	366	17	4	26	42	0	25	28	0	18	0	681	80	14	6	76	14	10	43	0	57
P-8	141	217	4	3	90	20	0	30	61	0	21	1	588	57	28	15	55	28	17	10	0	90
P-9	107	275	19	10	53	8	0	25	47	0	14	0	558	74	15	11	67	15	18	38	0	62
P-10	46	214	15	0	73	40	0	14	54	0	11	0	467	58	29	14	54	29	17	22	0	78
P-11	20	330	28	0	27	20	0	16	72	0	15	2	530	75	10	15	69	10	21	28	0	72
P-12	52	365	10	0	45	36	0	2	3	0	22	1	535	82	18	1	80	18	3	80	0	20
P-13	115	122	4	8	126	14	15	65	69	0	8	2	548	37	39	23	34	39	27	13	0	88
P-14	160	140	6	0	148	4	0	49	54	0	9	2	571	42	43	15	40	43	17	10	0	90
P-15	167	146	9	7	134	7	1	50	54	0	19	2	596	45	39	15	41	39	20	23	0	77
P-16	134	148	2	0	154	15	1	34	47	0	12	2	549	41	46	13	40	46	14	4	0	96
P-17	171	105	4	0	176	23	0	36	57	0	25	0	596	30	55	16	29	55	17	6.6	0	93
P-18	123	135	13	0	130	8	0	50	78	0	12	1	549	41	38	21	37	38	25	14	0	86
P-19	44	99	12	3	94	17	2	78	100	0	31	0	480	35	34	31	30	34	36	13	0	87
P-20	44	141	11	0	84	14	0	51	99	0	35	0	479	44	28	28	40	28	32	10	0	90
P-21	71	128	11	3	96	19	0	57	90	0	8	0	482	41	33	26	37	33	30	14	0	86
P-22	133	160	11	14	88	22	0	43	76	0	9	0	556	50	30	20	43	30	27	25	0	75
P-23	215	156	9	0	77	0	0	66	93	0	7	0	622	49	23	28	47	23	30	8.9	0	91
P-24	134	134	13	9	78	13	0	60	103	0	5	0	548	45	26	29	38	26	36	18	0	82
P-25	171	115	34	5	55	32	0	52	113	0	11	2	589	44	25	32	33	25	43	26	0	74
P-26	105	280	27	2	68	72	0	5	14	0	29	2	604	67	30	3	60	30	9	67	0	33
Profile P13 in Fig. 1B (35°17′22″N, 83°42′56″E)																						
P13-1	35	226	6	8	81	8	16	119	43	0	2	4	548	62	23	15	58	23	19	19	0	81
P13-2	53	186	43	0	42	15	0	68	166	0	23	0	596	51	13	37	41	13	46	21	0	79
P13-3	12	209	31	0	32	10	0	83	218	0	9	0	604	48	8	44	42	8	50	12	0	88
P13-4	39	210	6	0	44	8	0	121	58	5	11	0	502	65	16	19	63	16	21	8.7	7	84
P13-5	55	212	20	7	91	7	0	137	53	0	24	4	610	61	25	14	54	25	21	34	0	66
P13-6	93	244	13	0	89	14	47	5	73	0	6	2	586	54	21	25	51	21	28	9.8	0	90
P13-7	30	206	14	4	13	6	0	97	18	0	26	0	414	86	7	7	79	7	14	50	0	50
P13-8	89	227	20	3	61	12	0	103	182	0	19	1	717	50	14	36	45	14	41	11	0	89
P13-9	66	209	2	10	58	0	0	175	20	0	4	0	544	74	19	7	70	19	11	38	0	63
P13-10	30	183	17	0	110	50	0	73	94	0	13	0	570	44	35	21	40	35	24	15	0	85
P13-11	33	205	35	0	26	9	0	48	152	0	5	2	515	56	8	36	48	8	44	19	0	81
P13-12	56	175	8	0	74	4	0	80	157	0	23	1	578	44	19	38	42	19	39	4.8	0	95
P13-13	29	211	20	8	33	15	0	87	146	0	7	2	558	55	11	34	49	11	40	16	0	84
P13-14	28	221	6	0	17	9	0	144	56	0	2	2	485	73	8	18	72	8	20	9.7	0	90
P13-15	38	202	16	7	71	0	0	88	67	0	18	2	509	62	20	18	56	20	25	26	0	74
P13-16	47	234	40	0	60	21	0	133	93	0	4	2	634	61	18	21	52	18	30	30	0	70
P13-17	34	166	25	0	22	23	0	52	234	0	26	0	582	41	10	50	35	10	55	9.7	0	90
P13-18	68	216	27	0	66	21	0	124	100	0	22	1	645	57	20	23	50	20	30	21	0	79
P13-19	43	139	22	3	53	2	0	45	241	0	21	0	569	36	12	52	30	12	58	9.4	0	91
P13-20	70	169	7	0	101	4	0	50	135	0	40	0	576	42	25	32	41	25	34	4.9	0	95
P13-21	60	223	43	3	62	23	0	76	72	0	5	0	567	63	20	17	52	20	28	39	0	61
P13-22	32	221	14	14	97	23	0	138	46	0	4	0	589	60	29	11	53	29	18	38	0	62
P13-23	58	199	25	0	63	0	0	137	94	0	7	0	583	59	17	25	52	17	31	21	0	79
P13-24	36	216	18	9	18	6	0	171	90	0	0	0	564	68	7	25	61	7	33	23	0	77
P13-25	52	220	20	5	57	11	0	22	163	0	7	2	559	51	14	34	46	14	39	13	0	87
P13-26	44	217	0	2	91	0	0	164	79	0	17	2	616	56	23	20	56	23	21	2.5	0	98
P13-27	33	184	35	15	70	17	0	127	91	0	22	0	594	57	21	22	45	21	34	35	0	65
P13-28	66	220	19	0	94	8	0	61	181	0	24	0	673	46	20	35	42	20	38	9.5	0	91
Profile P2 in Fig. 1B (31°36′12″N, 99°56′5″E)																						
P2-9	64	260	13	8	31	16	0	22	85	0	11	5	515	68	11	21	63	11	26	20	0	80
P2-14	103	236	9	42	110	30	3	7	92	0	15	3	650	55	27	18	45	27	28	35	0	65
P2-15	41	255	26	20	16	35	0	132	95	0	23	0	643	67	11	21	57	11	32	33	0	67
P2-16	97	212	3	6	61	5	0	75	116	0	6	0	581	55	16	29	53	16	31	7.2	0	93
P2-17	71	220	6	59	77	11	0	10	33	0	0	1	488	70	22	8	54	22	24	66	0	34
P2-18	83	282	17	61	77	51	0	34	79	0	5	1	690	63	23	14	50	23	28	50	0	50

See Fig. 1B for the locations of the profiles.
Qm = monocrystalline quartz; Qp′ = polycrystalline quartz; Qp = Qp′ + chert; Q = Qm + Qp; F = plagioclase + K-feldspar; Ls = sedimentary lithic fragments (carbonate not included); Lv = volcanic lithic fragments; Lm = metamorphic lithic fragments; L = Ls + Lv + Lm; Lt = L + Qp; Lsm = (Ls + Lm)/(Qp + Chert + Ls + Lm + Lv) * 100.

eastern counterparts (average ~2%). In the two eastern profiles, the quartz content increases eastward from an average of 51% (profile P) to 56% (profile P2), whereas the feldspars and lithics decrease from 23% and 25% (profile P) to 18% and 18% (profileP2; Table 1).

4. Heavy-mineral spectra

The heavy-mineral spectra (n=8) of the analyzed sandstones are mostly dominated by zircon, (max. 77%; Table 2) followed by rutile

Table 2
Heavy-mineral data of the analyzed samples (%)

Sample	Rutile	Tourmaline	Zircon	Apatite	Garnet	Amphibole	Chrome spinel	Chlorite	Pyroxene	Epidote
Profile P in Fig. 1B (33°07′06″N, 97°20′02″E)										
P-1	13.5	1.0	71.5	n.d.	2.8	3.2	1.2	3.8	2.0	n.d.
P-2	9.8	1.4	61.5	0.5	8.0	9.3	1.5	4.2	3.3	0.5
P-3	15.0	1.2	70.6	n.d.	3.4	3.5	0.5	3.5	1.8	0.5
Profile P2 in Fig. 1B (31°36′12″N, 99°56′5″E)										
P2-1	8.5	1.7	76.9	1.2	5.5	2.1	0.5	2.6	1.0	n.d.
P2-2	9.0	1.8	72.1	0.8	5.2	4.3	1.9	2.3	1.8	0.9
Profile P13 in Fig. 1B (35°17′22″N, 83°42′56″E)										
P13-1	15.5	1.0	49.1	n.d.	13.2	8.4	2.0	4.3	5.5	1.0
P13-2	18.3	1.5	47.7	0.5	6.3	7.8	4.4	8.2	3.8	1.5
P13-3	11.7	2.3	53.5	0.8	9.8	7.4	1.8	6.5	4.9	1.3

"n.d." represents "not detected".

and garnet (Fig. 7). Chemically ultrastable zircons occur predominantly as unabraded grains (Fig. 5G–I). The shapes and lack of abrasion of zircons indicate that long-distance transport is very unlikely. The garnets are pink and subhedral (Fig. 5C). All the analyzed garnet grains are homogeneous and lack zoning. Microprobe analyses yield garnet compositions of $Alm_{56\pm9}And_{1\pm1}Grs_{11\pm7}Prp_{20\pm9}Sps_{12\pm10}$ (Table 1 in the Online supplementary data), and they locate within the Group C eclogite field of Coleman et al. (1965) (Fig. 6B). Garnet composition could be consistent with an eclogitic source, but also could be consistent with slightly lower-grade/pressure metamorphic rocks. One Si-rutile grain that is made up almost entirely of TiO_2 and SiO_2 was detected in profile P13 (73.8 wt.%, 26.8 wt.%, respectively. Table 1 in the Online supplementary data). Chrome spinel grains are rare, and they have Cr# values (Cr/(Cr+Al)) of less than 0.6, indicating a likely derivation from a Mid-Ocean Ridge setting (Dick and Bullen, 1984). Kamenetsky et al. (2001) pointed out that, using an Al_2O_3 vs. TiO_2 diagram of spinel compositions, the mid-ocean ridge, ocean island, large igneous province, and island-arc settings can be well distinguished with little overlap. A plot on the wt.% Al_2O_3 vs. TiO_2 diagram of Kamenetsky et al. (2001) is consistent with the above-mentioned conclusion. Pyroxenes are predominantly Ca–Mg–Fe pyroxenes, and only one omphacite grain was analyzed from profile P (Fig. 5D), with ~40% jadeite (Fig. 6A; Table 1 in the Online supplementary data). Amphiboles (Fig. 5B) are prevailingly Ca–Mg–Fe amphiboles of the greenschist and epidote–amphibole facies (Fig. 6D; Table 1 in the Online supplementary data) and contain actinolite, cummingtonite, eckrite, and hornblende. The actinolite is dominant (Table 1 in the Online supplementary data). Chlorite is a common detrital mineral (Fig. 5F). In addition, epidote is also present in the sandstone samples (Fig. 5E; Table 1 in the Online supplementary data). The irregular and fragmentary morphologies of the low-grade metamorphic detrital minerals, such as chlorite and albite, as well as their inharmonious relations with the matrix, make it clear that they could not be in situ neogenic minerals. In fact, the metamorphic grade of the turbidite in the study area is zeolite- to pumpellyite-facies as pointed out before, and there is no in situ neogenic chlorite and albite in the studied samples.

5. Discussion

Upper Triassic turbidites in western Songpan–Ganzi seem to have an overwhelming derivation from an orogen source, as shown by the framework compositions of the sandstones (Fig. 4). Both the light and heavy mineral and lithic fractions indicate the overwhelming importance of metamorphic source rocks. Chrome spinel is a ubiquitous accessory phase in several types of ultramafic and mafic rocks and is generally thought to indicate an oceanic crustal provenance (e.g., Dick and Bullen, 1984). Amphiboles are common and are restricted to magmatic and metamorphic source rocks. Scarcity of high-pressure amphiboles is attributed to their relative instability with respect to both physical and chemical abrasion and high sensitivity to intrastratal dissolution (Morton, 1985; Morton and Hallsworth, 1994). Si-

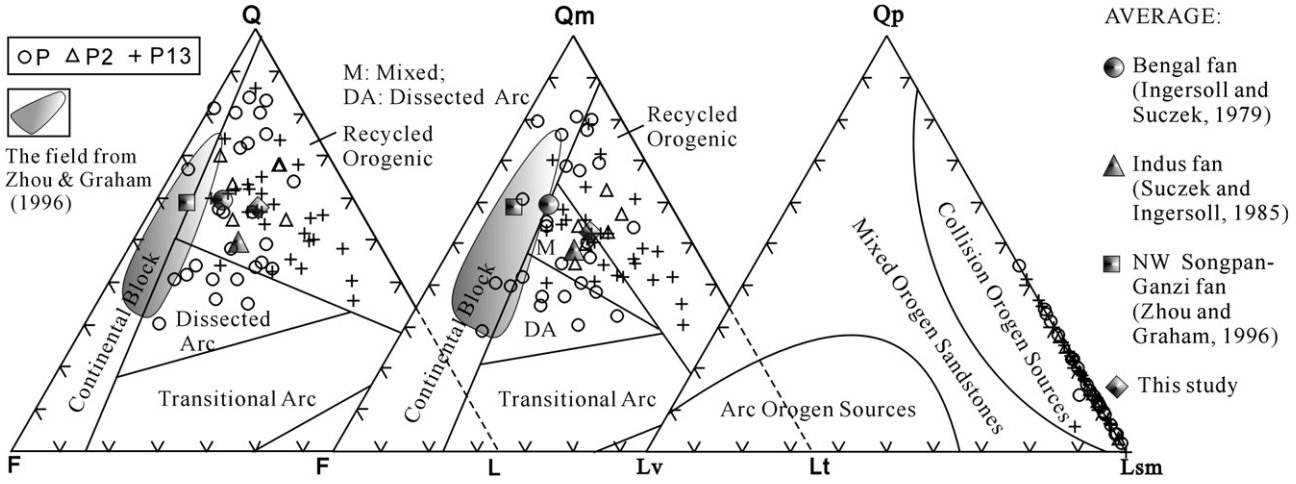

Fig. 4. Ternary plots of modal sandstone grain compositions in the Songpan-Ganzi complex (see Table 1 for data employed). Provenance associations were proposed by Dickinson et al. (1983). *L*—total lithic fragments, *Lsm*—sedimentary and metamorphic lithic fragments, *Lt*—total lithic fragments+polycrystalline quartz, *Lv*—volcanic lithic fragments, *P*—plagioclase, *Q*—quartz, *Qm*—monocrystalline quartz, *Qp*—polycrystalline quartz.

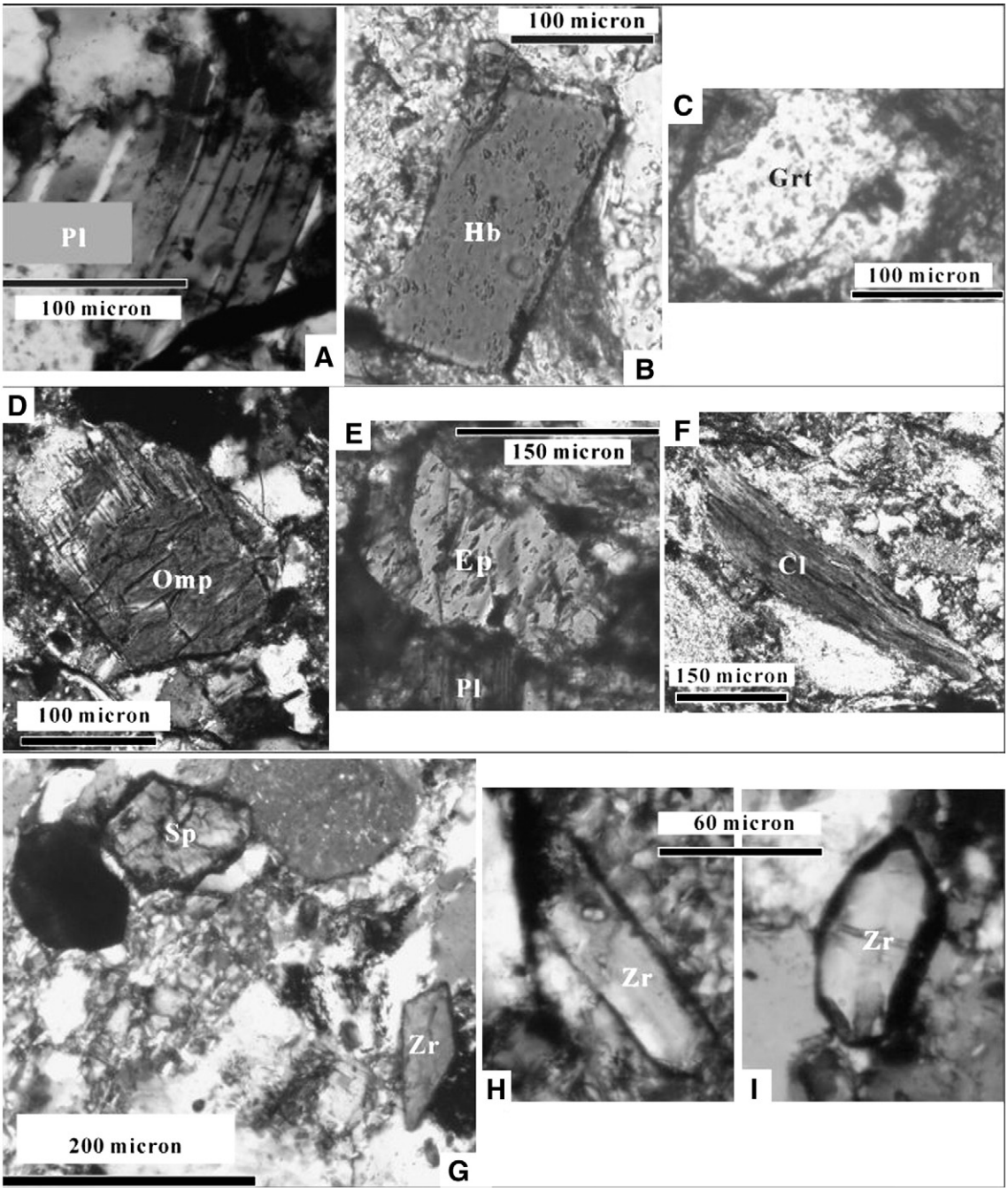

Fig. 5. Photos characterizing the accessory minerals/heavy minerals of the sandstones from Triassic flysch sequence in the western Songpan–Ganzi complex. Photos A, D, E were taken from profile P13; B, C, F from profile P; G, H, I from profile P2. Abbreviations: *Cl*—chlorite, *Ep*—episode, *Grt*—garnet, *Hb*—amphibole, *Pl*—plagioclase, *Omp*—omphacite, *Sp*—Sphene, *Zr*—zircon. Photos B and C with single polar and others with crossed polars.

rutile was first reported in the Luobusha UHP terrane along the Yarlung Zangbo suture of southern Tibet, in a close intergrowth with UHP minerals such as octahedral silicate, silicon–magnesium spinel, and diamond. The Si^{4+} ions in Si-rutile are six-coordinated (^{VI}Si), which can be achieved only at very high pressure (e.g., Knittle and Jeanloz, 1989), and Si-rutile was thus believed to be a typical UHP mineral that is probably originated from the transition zone or the lower mantle (Yang et al., 2003). Epidote occurs in a variety of metamorphic rocks but is particularly common in rocks of the greenschist and epidote–amphibolite facies (Deer et al., 1992). It also occurs in rocks formed at high pressures (e.g. blueschists and amphibolized eclogites; Deer et al., 1992). Garnet-group minerals are common in heavy-mineral spectra of siliciclastic sediments and are generally interpreted to indicate metamorphic source rocks (Deer et al., 1992). The occurrence of C-type garnet (Coleman et al., 1965), omphacite, rutile (Green and Ringwood, 1967), and Si-rutile (Yang et al., 2003), and the high-silica contents in phengite (Massone and Schreyer, 1987), suggest that the source rocks underwent ultrahigh-pressure conditions.

In addition, the immaturity of both composition and texture of the sandstones suggests limited transport and a nearby source. The Triassic turbidites in the northeastern Songpan–Ganzi corner could possibly have been derived from erosion of mainly the Qinling–Dabie orogen that includes both the metamorphic orogenic core and uplifted sedimentary rocks of the fold-thrust belt, as indicated by sandstone compositions (Zhou and Graham, 1996), paleocurrents

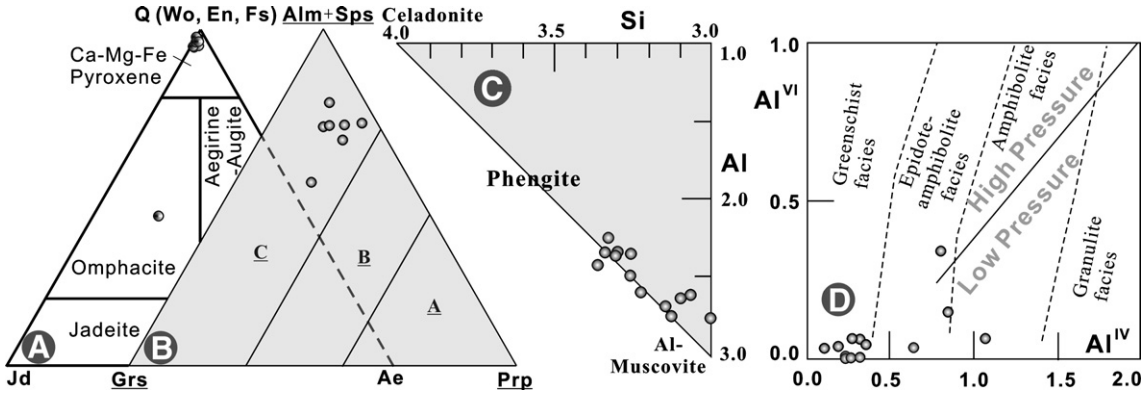

Fig. 6. Representative pyroxene (A), garnet (B), phengite (C), and amphibole (D) compositions from the sandstones (see Table 1 in the Online supplementary data for data employed). (A), (B), and (D) plotted after Morimoto et al. (1988), Coleman et al. (1965), and Rasse (1974), respectively. In B, field A represents garnets in eclogite inclusions in kimberlites, basalts, or ultramafic rocks with >55% pyrope, field B represents garnets in bands or lenses of eclogite within migmatite gneissic terrains with 30–55% pyrope, and field C represents garnets in bands or lenses of eclogite within alpine-type metamorphic rocks with <30% pyrope (Coleman et al., 1965). Abbreviations: *Q*—quadrilateral pyroxene, *Ae*—aegirine, *Alm*—almandine, *En*—enstatite, *Fs*—ferrosilite, *Grs*—grossular, *Jd*—jadeite, *Prp*—pyrope, *Sps*—spessartine, *Wo*—wollastonite.

(Zhou and Graham, 1996; Weislogel et al., 2006), and detrital zircon ages (Weislogel et al., 2006). However, we argue that the Late Triassic turbidites in western Songpan–Ganzi were not sourced from the Qinling–Dabie orogen as in the northeastern counterpart, but instead were most likely derived from the central Qiangtang UHP orogen, based on following reasons. (1) Occurrence of typical high-pressure minerals such as garnet, omphacite, rutile, and phengite in our sandstone samples indicates that they should have been deposited more proximally to their source areas than their northeastern counterparts. In the latter, no high-pressure relics were observed, which forms a major obstacle for the Dabie UHP rocks as the only source rocks of the Songpan–Ganzi turbidites (Avigad, 1995). (2) Compared with those in the northeastern Songpan–Ganzi corner studied by Zhou and Graham (1996), our sandstone samples contain lesser amounts of stable compositions (average 57% quartz grains) but more abundant instable contents (average 21% and 22% of feldspar and lithic fragments, respectively) (Fig. 4). (3) The paleocurrents indicate that the prevailing transport directions of the sediments were easterly (Fig. 1B). In summary, it is very unlikely that the sediments in western Songpan–Ganzi (dominantly orogen-derived, Fig. 4) were transported through its northeastern corner (continental block-derived, Zhou and Graham, 1996. Fig. 4), because if so the stable components in the western Songpan–Ganzi sandstones should have been apparently more than those in their northeastern counterparts, after abrasion and weathering through transport of far more than 500 km.

Central Qiangtang contains distinct high-pressure eclogites (Zhang et al., 2006a) and blueschists (e.g. Kapp et al., 2000, 2003) and marks an in situ suture separating eastern and western Qiangtang (Shuanghu suture. Fig. 1A; Zhang, 2001a; Zhang et al., 2006a,b, 2007). The denudation of the central Qiangtang UHP metamorphic rocks is comparable in volume (~2.5×10^6 km^3. Zhang et al., 2006a) to the Upper Triassic flysch rocks in the Songpan–Ganzi region (~2×10^6 km^3, Nie et al., 1994). Limited age data from the central Qiangtang metamorphic rocks suggest that they were possibly exhumed at ~220–202 Ma (Kapp et al., 2003; Zhang et al.,

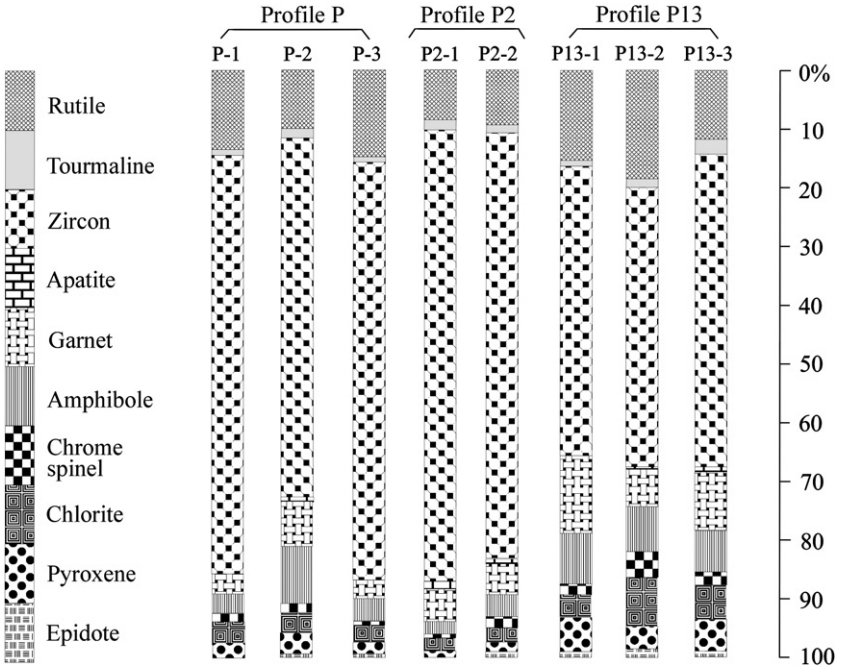

Fig. 7. Spatial distribution of the heavy-mineral spectra of Upper Triassic sandstones in western Songpan–Ganzi (See Table 2 for data used).

2006a). However, other studies on the Qiangtang Mesozoic sandstones apparently reveal that the exhumation could have been initiated earlier, and most likely since the beginning of the Late Triassic (230 Ma) based on the extensive distribution of metamorphic lithic fragments and diagnostic metamorphic minerals (e.g., amphibole, chlorite, chrome spinel, epidote, garnet, rutile) in Upper Triassic sandstones (Zhang et al., 2006c). Therefore, this exhumation correlates well with the main interval in which the Songpan–Ganzi turbidites accumulated, and thus could have provided a major source for these sedimentary rocks in the western Songpan–Ganzi terrane (Zhang et al., 2006a). This area must then have contained fragments of ophiolitic complexes, which constitute the source rocks for chert, chrome spinel, pyroxene, and amphibole. Upper Triassic rocks are lacking in the majority of Qiangtang (Ruo et al., 1987; GSC and CIGMR, 2004) and abundance in dense minerals such as rutile, garnet, chrome spinel, pyroxene, amphibole, chlorite, and epidote in Upper Triassic–Lower Jurassic sandstones in Qiangtang (Zhang et al., 2006c) favors a mixed source from nearby (high pressure) metamorphic and ultramafic–mafic rocks, and thus supports the above conclusions.

Potassium feldspar also indicates minor acid plutonic source rocks. The Yidun arc is a likely source but the paucity of volcanic fragments in the sandstones does not favor it as a significant sediment supply. In addition, the Yidun arc was dominated by interbedded andesites and shallow-marine carbonate and clastic rocks during Late Triassic time (Ruo et al., 1987; Hou et al., 1991) and thus could not have been the main source area (Nie et al., 1994). The acid plutonic compositions that are represented by the potassium feldspar are thus to be expected for sand eroded from the deeply exhumed orogen (Zhou and Graham, 1996). Erosional unroofing of carbonate cover strata of the central Qiangtang orogen could have also formed a minor source for the sediments. Therefore, the greatest likelihood appears to be a mixed provenance that includes both the metamorphic orogen core and uplifted sedimentary rocks of the fold-thrust belt, which has important implications for tectonic reconstructions and paleogeographic reconstructions of the area.

6. Conclusions

Although slightly metamorphosed to zeolite- to pumpellyite-grade, Upper Triassic sandstones of the western Songpan–Ganzi turbidite complex of the eastern Tibetan plateau can still provide key constraints on their source areas. The wealth of labile metamorphic lithic and dense mineral fragments in the sandstones indicates that petrography has not been drastically affected by weathering or diagenesis. They are immature both compositionally and texturally, and are mostly first-cycle sandstones derived from high-pressure metamorphic rocks, and subordinate ophiolitic and sedimentary rocks. Clearly, they were derived from nearby central Qiangtang Triassic collisional orogen sources, rather than the distant Dabie–Qinling sources eroded after the North China–South China collision, as previously proposed.

Our findings have significant implications for the tectonic amalgamation and paleogeographic reconstructions of China. The probability that the central Qiangtang metamorphic belt, as a contributor of the Songpan–Ganzi flysch, occurred as an early Mesozoic mélange underthrust from the Jinsa suture (Kapp et al., 2000, 2003) seems unlikely. It is more likely to have been an in situ Triassic ultrahigh-pressure orogen between northern and southern Qiangtang (Zhang, 2001a; Zhang et al., 2006a,b,c, 2007). In addition, the analogy of the Songpan–Ganzi turbidites to the Bengal–Indus fans, that hypothesized that they were only fed by single orogens (the former by the Dabie–Qinling orogen and the latter by the Himalayan orogen; e.g., Nie et al., 1994; Weislogel et al., 2006), is not favored by this study. The Songpan–Ganzi turbidites were possibly accumulated clearly from multi-sources (Bruguier et al., 1997; She et al., 2006; Weislogel et al., 2006), and the central Qiangtang orogen must have been a major contributor. Moreover, the Paleotethys, represented by the present Jinsa and Kunlun sutures on the southern and northern sides of the Songpan–Ganzi basin, respectively (Fig. 1A), was not yet closed when the central Qiangtang ultrahigh-pressure orogen was being exhumed to supply the sediments of the basin. This challenges the conventional model for the tectonic amalgamation of China, in which China was generally believed to be a product of sequential amalgamation of southerly terranes during the Phanerozoic (see Huang and Chen, 1987; GSC and CIGMR, 2004; and references therein).

Acknowledgements

This research was supported by Chinese Academy of Sciences. We thank Lin-Li Chen for analytical assistance, and Amy L. Weislogel, Gert J. Weltje, and an anonymous reviewer for constructive and thoughtful comments as well as generous editorial help, which greatly improved the manuscript.

Appendix A. Supplementary data

Supplementary data associated with this article can be found, in the online version, at doi:10.1016/j.sedgeo.2008.04.008.

References

Avigad, D., 1995. Exhumation of the Dabie Shan ultra-high-pressure rocks and accumulation of the Songpan–Ganzi flysch sequence, central China: Discussion. Geology 23, 764–765.
Bruguier, O., Lancelot, J.R., Malavieille, J., 1997. U–Pb dating on single detrital zircon grains from the Triassic Songpan–Ganze Flysch (central China): provenance and tectonic correlations. Earth Planet. Sci. Lett. 152, 217–231.
Coleman, R.G., Lee, D.E., Beatty, L.B., Brannock, W.W., 1965. Eclogites: their differences and similarities. Geol. Soc. Amer. Bull. 76, 483–508.
Deer, W.A., Howie, R.A., Zussman, J., 1992. An Introduction to Rock-forming Minerals, Orthosilicates, Second edition. Longman, New York.
Dick, H.J.B., Bullen, T., 1984. Chromian spinel as a petrogenetic indicator in abyssal and alpine-type peridotite and spatially associated lavas. Contrib. Mineral. Petrol. 86, 54–76.
Dickinson, W.R., Beard, L.S., Brakenridge, G.R., Erjavec, J.L., Ferguson, R.C., Inman, K.F., Knepp, R.A., Lindberg, F.A., Ryberg, P.T., 1983. Provenance of North American Phanerozoic sandstones in relation to tectonic setting. Geol. Soc. Amer. Bull. 94, 222–235.
Green, D.H., Ringwood, A.E., 1967. An experimental investigation of the grabbo to eclogite transformation and its petrological applications. Geochim. Cosmochim. Acta 31, 767–833.
GSC (Geological Survey of China) and CIGMR (Chengdu Institute of Geology and Mineral Resources), 2004. Geological map of Tibet (China) and adjacent areas (1: 1,500,000) with an explanation. Chengdu, Chengdu Cartographic Press.
Gu, X.X., 1994. Geochemical characteristics of the Triassic Tethys-turbidites in northwestern Sichuan, China: Implications for provenance and interpretations of the tectonic setting. Geochim. Cosmochim. Acta 58, 4615–4631.
Hou, L.W., Luo, D.X., Fu, D.M., Hu, S.H., Li, K.Y., 1991. Triassic Sedimentary– tectonic Evolution in Western Sichuan and Eastern Xizang (Tibet) Regions. Geological Publishing House, Beijing.
Huang, J.Q., Chen, B.W., 1987. The Evolution of the Tethys in China and Adjacent Regions. Geological Publishing House, Beijing.
Ingersoll, R.V., Suczek, C.A., 1979. Petrology and provenance of Neogene sand from Nicobar and Bengal fans, DSDP sites 211 and 218. J. Sediment. Petrol. 49, 1217–1228.
Ingersoll, R.V., Bullard, T.F., Ford, R.L., Grimm, J.P., Pickle, J.D., Sares, S.W., 1984. The effect of grain size on detrital modes: a test of the Gazzi–Dickinson point counting method. J. Sediment. Petrol. 54, 103–116.
Kamenetsky, V.S., Crawford, A.J., Meffre, S., 2001. Factors controlling chemistry of magmatic spinel: an empirical study of associated olivine, Cr-spinel and melt inclusions from primitive rocks. J. Petrol. 42, 655–671.
Kapp, P., Yin, A., Manning, C.E., Murphy, M., Harrison, T.M., Spurlin, M., Ding, L., Deng, X.G., Wu, C.M., 2000. Blueschist-bearing metamorphic core complexes in the Qiangtang block reveal deep crustal structure of northern Tibet. Geology 28, 19–22.
Kapp, P., Yin, A., Manning, C.E., Harrison, T.M., Taylor, M.H., 2003. Tectonic evolution of the early Mesozoic blueschist-bearing metamorphic belt, central Tibet. Tectonics 24, 1043. doi: 1029/2002TC001383.
Knittle, E., Jeanloz, R., 1989. Simulating the core–mantle boundary: An experimental study of high-pressure reactions between silicates and liquid iron. Geophys. Res. Lett. 16, 609–612.
Mange, M.A., Maurer, H.F.W., 1992. Heavy Minerals in Color. Chapman and Hall, London.
Massone, H.J., Schreyer, W., 1987. Phengite barometry based on the limiting assemblage with K-feldspar, phlogopite and quartz. Contrib. Mineral. Petrol. 96, 212–224.
Morimoto, N., Fabries, J., Ferguson, A.K., Ginzburg, I.V., Ross, M., Seifert, F.A., Zussman, J., Aoki, K., Gottardi, G., 1988. Nomenclature of pyroxenes. Am. Mineral. 73, 1123–1133.

Morton, A.C., 1985. Heavy minerals in provenance studies. In: Zuffa, G.G. (Ed.), Provenance of Arenites. Reidel, Dordrecht.
Morton, A.C., Hallsworth, C., 1994. Identifying provenance-specific features of detrital heavy mineral assemblages in sandstones. Sediment. Geol. 90, 241–256.
Najman, Y., 2006. The detrital record of orogenesis: A review of approaches and techniques used in the Himalayan sedimentary basins. Earth-Sci. Rev. 74, 1–72.
Nie, S., Yin, A., Rowley, D.B., Jin, Y., 1994. Exhumation of the Dabie Shan ultrahigh-pressure rocks and accumulation of the Songpan–Ganzi flysch sequence, central China. Geology 22, 999–1002.
Rasse, P., 1974. Al and Ti contents of hornblende, indicators of pressure and temperature of regional metamorphism. Contrib. Mineral. Petrol. 45, 231–236.
Ruo, R.B., Xu, J.F., Chen, Y.M., Zou, D.B., 1987. The Triassic System of the Qinghai–Xizang (Tibet) Plateau. Geological Publishing House, Beijing.
Ryburn, R.J., Råheim, A., Green, D.H., 1976. Determination of the P, T paths of natural eclogites during metamorphism: a record of subduction. A correction. Lithos 9, 161–165.
She, Z.B., Ma, C.Q., Mason, R., Li, J.W., Wang, G.C., Lei, Y.H., 2006. Provenance of the Triassic Songpan–Ganzi flysch, west China. Chem. Geol. 231, 159–175.
Suczek, C.A., Ingersoll, R.V., 1985. Petrology and provenance of Cenozoic sand from the Indus cone and the Arabian basin, DSDP sites 221, 222, and 224. J. Sediment. Petrol. 55, 340–345.
Weislogel, A.L., Graham, S.A., Chang, E.Z., Wooden, J.L., Gehrels, G.E., Yang, H.S., 2006. Detrital zircon provenance of the Late Triassic Songpan–Ganzi complex: Sedimentary record of collision of the North and South China blocks. Geology 34, 97–100.
Yang, J.S., Bai, W.J., Fang, Q.S., Yan, B.G., Shi, N.C., Ma, Z.S., Dai, M.Q., Xiong, M., 2003. Silicon–rutile — an ultra-high pressure (UHP) mineral from an ophiolite. Prog. Nat. Sci. 13, 528–531.
Zhang, K.J., 2001a. Blueschist-bearing metamorphic core complexes in the Qiangtang block reveal deep crustal structure of northern Tibet: Comment. Geology 29, 90.
Zhang, K.J., 2001b. Is the Songpan–Ganzi terrane (central China) really underlain by oceanic crust? J. Geol. Soc. India 57, 223–230.
Zhang, K.J., 2002. Escape hypothesis for the North and South China collision and the tectonic evolution of the Qinling orogen, eastern Asia. Eclogae Geol. Helv. 95, 237–247.
Zhang, K.J., Cai, J.X., Zhang, Y.X., Zhao, T.P., 2006a. Eclogites from central Qiangtang, northern Tibet (China) and tectonic implications. Earth Planet. Sci. Lett. 245, 722–729.
Zhang, K.J., Zhang, Y.X., Li, B., Zhu, Y.T., Wei, R.Z., 2006b. The blueschist-bearing Qiangtang metamorphic belt (northern Tibet, China) as an in situ suture zone: Evidence from geochemical comparison with the Jinsa suture. Geology 34, 493–496.
Zhang, K.J., Zhang, Y.X., Xia, B.D., He, Y.B., 2006c. Temporal variations of the Mesozoic sandstone composition in the Qiangtang block, northern Tibet (China): Implications for provenance and tectonic setting. J. Sediment. Res. 76, 1035–1048.
Zhang, K.J., Cai, J.X., Zhu, J.X., 2006d. North China and South China collision: insights from analogue modeling. J. Geodyn. 42, 38–51.
Zhang, K.J., Zhang, Y.X., Li, B., Zhong, L.F., 2007. Nd isotopes of siliciclastic rocks from Tibet: Constraints on the pre-Cenozoic tectonic evolution. Earth Planet. Sci. Lett. 256, 604–616.
Zhou, D., Graham, S.A., 1996. Songpan–Ganzi Triassic flysch complex of the West Qinling Shan as a remnant ocean basin. In: Yin, A., Harrison, M. (Eds.), The Tectonic Evolution of Asia. Cambridge University Press, Cambridge, pp. 281–299.